

# Synthesis and Coordination Properties of Trifluoromethyl Decorated Derivatives of 2,6-Bis[(diphenylphosphinoyl)methyl]pyridine N-Oxide Ligands with Lanthanide Ions

Sylvie Pailloux,<sup>†</sup> Cornel Edicome Shirima,<sup>†</sup> Alisha D. Ray,<sup>†</sup> Eileen N. Duesler,<sup>†</sup> Robert T. Paine,<sup>\*,†</sup> John R. Klaehn,<sup>‡</sup> Michael E. McIlwain,<sup>‡</sup> and Benjamin P. Hay<sup>§</sup>

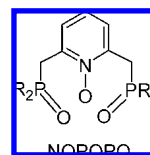
Department of Chemistry and Chemical Biology, University of New Mexico, Albuquerque, New Mexico 87131, Idaho National Laboratory, P.O. Box 1625, Idaho Falls, Idaho 83415, and Oak Ridge National Laboratory, P.O. Box 2008, Oak Ridge, Tennessee, 37831

Received December 15, 2008

Phosphinoyl Grignard-based substitutions on 2,6-bis(chloromethyl)pyridine followed by N-oxidation of the intermediate 2,6-bis(phosphinoyl)methylpyridine compounds with *m*CPBA give the target trifunctional ligands 2,6-bis[bis(2-trifluoromethylphenyl)phosphinoylmethyl]pyridine 1-oxide (**2a**) and 2,6-bis[bis(3,5-bis(trifluoromethyl)phenyl)phosphinoylmethyl]pyridine 1-oxide (**2b**) in high yields. The ligands have been spectroscopically characterized, the molecular structures confirmed by single crystal X-ray diffraction methods, and the coordination chemistry surveyed with lanthanide nitrates. Single crystal X-ray diffraction analyses are described for the coordination complexes Nd(**2a**)(NO<sub>3</sub>)<sub>3</sub>, Nd(**2a**)(NO<sub>3</sub>)<sub>3</sub> · (CH<sub>3</sub>CN)<sub>0.5</sub>, Eu(**2a**)(NO<sub>3</sub>)<sub>3</sub>, and Nd(**2b**)(NO<sub>3</sub>)<sub>3</sub> · (H<sub>2</sub>O)<sub>1.25</sub>; in each case the ligand binds in a tridentate mode to the Ln(III) cation. These structures are compared with the structures found for lanthanide coordination complexes of the parent NOPOPO ligand, [Ph<sub>2</sub>P(O)CH<sub>2</sub>]<sub>2</sub>C<sub>5</sub>H<sub>3</sub>NO.

## Introduction

In previous reports,<sup>1–6</sup> we have documented the synthetic development of bis(phosphinoylmethyl)pyridine 1-oxides,<sup>7</sup> [R<sub>2</sub>P(O)CH<sub>2</sub>]<sub>2</sub>C<sub>5</sub>H<sub>3</sub>NO, (NOPOPO), (R = alkyl or aryl). These compounds act as neutral, tridentate chelating ligands that form stable 1:1 and 2:1 (L:M) complexes with lanthanide, Ln(III),<sup>1,3–6,8</sup> Th(IV)<sup>1</sup> and Pu(IV)<sup>9</sup> ions.



In addition, the ligands display favorable performance as liquid–liquid extractants of trivalent Ln(III) and actinide, An(III), ions present in strongly acidic aqueous solutions,<sup>6,10–12</sup> an unusual characteristic shared only with carbamoylmethyl phosphonates (CMP) and carbamoylmethyl phosphine oxides (CMPO).<sup>13–16</sup> The NOPOPO ligand extraction performance was initially assessed with the tetraphenyl derivative, R = Ph, in chlorinated hydrocarbon

\* To whom correspondence should be addressed. E-mail: rtpaine@unm.edu.

<sup>†</sup> University of New Mexico.

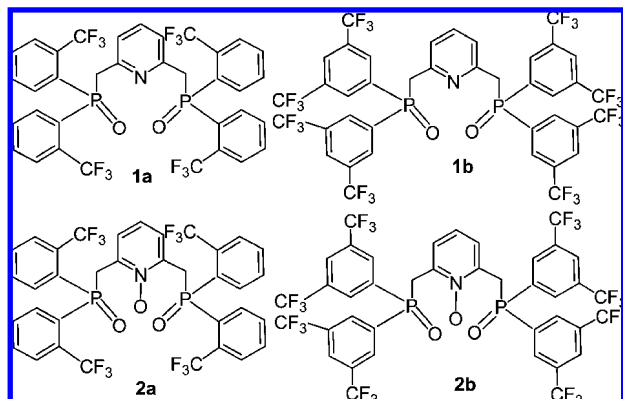
<sup>‡</sup> Idaho National Laboratory.

<sup>§</sup> Oak Ridge National Laboratory.

- (1) Rapko, B. M.; Duesler, E. N.; Smith, P. H.; Paine, R. T.; Ryan, R. R. *Inorg. Chem.* **1993**, *32*, 2164.
- (2) Engelhardt, U.; Rapko, B. M.; Duesler, E. N.; Frutos, D.; Paine, R. T.; Smith, P. H. *Polyhedron* **1995**, *14*, 2361.
- (3) Gan, X.; Duesler, E. N.; Paine, R. T. *Inorg. Chem.* **2001**, *40*, 4420.
- (4) Gan, X.; Paine, R. T.; Duesler, E. N.; Nöth, H. *Dalton Trans.* **2003**, 153.
- (5) Gan, X.; Rapko, B. M.; Duesler, E. N.; Binyamin, I.; Paine, R. T.; Hay, B. P. *Polyhedron* **2005**, *24*, 469.
- (6) Nash, K. L.; Lavalette, C.; Borkowski, M.; Paine, R. T.; Gan, X. *Inorg. Chem.* **2002**, *41*, 5849.
- (7) In prior publications these compounds have been named as bis(phosphinomethyl)pyridine N,P,P'-trioxides. The nomenclature has been revised to meet current rules.
- (8) Bond, E. M.; Duesler, E. N.; Paine, R. T.; Nöth, H. *Polyhedron* **2000**, *19*, 2135.

- (9) Matonic, J. H.; Neu, M. P.; Enriquez, A. E.; Paine, R. T.; Scott, B. L. *Dalton Trans.* **2002**, 2328.
- (10) Bond, E. M.; Engelhardt, U.; Deere, T. P.; Rapko, B. M.; Paine, R. T.; FitzPatrick, J. R. *Solv. Extr. Ion Exch.* **1997**, *15*, 381.
- (11) Bond, E. M.; Engelhardt, U.; Deere, T. P.; Rapko, B. M.; Paine, R. T.; FitzPatrick, J. R. *Solv. Extr. Ion Exch.* **1998**, *16*, 967.
- (12) Bond, E. M.; Gan, X.; FitzPatrick, J. R.; Paine, R. T. *J. Alloys Compd.* **1998**, *271–273*, 172.
- (13) Horwitz, E. P.; Kalina, D. G.; Kaplan, L.; Mason, G. W.; Diamond, H. *Sep. Sci. Technol.* **1982**, *17*, 1261.
- (14) Kalina, D. G.; Horwitz, E. P.; Kaplan, L.; Muscatello, A. C. *Sep. Sci. Technol.* **1981**, *16*, 1127.

solvent.<sup>10–12</sup> However, chlorinated solvents are unacceptable in process scale operations; therefore, a dodecane soluble derivative ( $R = 2\text{-EtHx}$ ) was produced and its extraction properties characterized.<sup>6</sup> During the course of these studies a new multicomponent extraction process (the Universal extraction, UNEX) was devised for simultaneous extraction of Cs, Sr, and An ions from acidic solutions. This employs  $\text{Ph}_2\text{P}(\text{O})\text{CH}_2\text{C}(\text{O})\text{N}(\text{n-Bu})_2$  as the actinide extractant<sup>17–19</sup> and phenyl trifluoromethyl sulfone (FS-13) as the diluent solvent. The process provides for excellent separations performance when small concentrations of Ln and An ions are present; however, because of modest CMPO solubility and low metal–ligand complex solubility in FS-13, the system has limited utility when Ln and An concentrations are high.<sup>20</sup> This issue has stimulated interest in the development of related new compositions that provide comparable or higher ligand solubility in FS-13, as well as improved aqueous/organic phase partitioning. Addition of trifluoromethyl groups to a molecule can promote its solubility in a fluorinated solvent such as FS-13; therefore, in the present study the initial objective was to determine if the organic framework of NOPOPO-type extractants could be decorated with  $\text{CF}_3$  substituents. The specific compounds of interest are shown here. Once available for study, the next objective was to determine the solubility of **2a** and **2b** in FS-13 and assess the effects of  $\text{CF}_3$  substitution on the coordination behavior of the ligands toward Ln(III) ions.



## Experimental Section

**General Information.** The organic reagents for the syntheses were purchased from Aldrich Chemical Co. and used without purification unless noted otherwise, and organic solvents were

obtained from VWR. THF was dried and distilled using standard procedures. The  $\text{Eu}(\text{NO}_3)_3 \cdot 5\text{H}_2\text{O}$  was obtained from Aldrich Ventron, and the  $\text{Nd}(\text{NO}_3)_3 \cdot 5\text{H}_2\text{O}$  from Aldrich. Infrared spectra were recorded on a Bruker Tensor 27 benchtop spectrometer; solution NMR spectra were measured (20 °C) on a Bruker FX-250 spectrometer. The NMR standards were TMS ( $^1\text{H}$ ,  $^{13}\text{C}$ ) and 85%  $\text{H}_3\text{PO}_4$  ( $^{31}\text{P}$ ), and downfield shifts were assigned as  $+\delta$ . Elemental analyses were obtained from Galbraith Laboratories. Mass spectra were obtained from the University of New Mexico Mass Spectrometry Facility.

**Ligand Synthesis.** 2,6-Bis(chloromethyl)pyridine was prepared as described previously.<sup>21</sup> **Caution!** This reagent and its solutions should be handled in a well-ventilated fume hood. Skin and eye contact must be carefully avoided since the compound is an aggressive skin and bronchial irritant with variable individual response symptoms.

**2,6-Bis[bis(2-(trifluoromethyl)phenyl)phosphinoylmethyl]pyridine (1a).** A solution of 2-bromobenzotrifluoride (5.7 mL, 42.0 mmol) in dry tetrahydrofuran (THF, 42 mL) was combined dropwise with a suspension of magnesium (1.0 g, 42.0 mmol) in dry THF (10 mL). The temperature rose during the addition. Following addition, the mixture was stirred (1 h), then cooled to 23 °C, and a solution of diethylphosphite (1.45 mL, 11.0 mmol) in dry THF (20 mL) was added dropwise. The mixture was refluxed (1 h), then cooled (23 °C). A solution of 2,6-bis(chloromethyl)-pyridine (1.0 g, 5.7 mmol) in dry THF (20 mL) was added dropwise at 23 °C, and the mixture stirred and refluxed (12 h). The resulting mixture was quenched with a saturated aqueous solution of  $\text{NH}_4\text{Cl}$  (100 mL), the aqueous phase was separated, and then extracted with  $\text{CH}_2\text{Cl}_2$  ( $3 \times 20$  mL). The organic phases were combined, dried over  $\text{Na}_2\text{SO}_4$  and concentrated. A crude solid was obtained (4.0 g, 90%), that was recrystallized from methanol to give a white solid, **1a**: yield 3.7 g, 84%; mp 180–182 °C. IR (KBr,  $\text{cm}^{-1}$ ): 3076 (w), 1585 (s), 1448 (s), 1397 (w), 1315 (vs), 1271 (s), 1179 (vs), 1120 (vs), 1035 (s), 959 (w), 894 (w), 839 (vw), 818 (w), 776 (s), 710 (s), 641 (w), 592 (s), 556 (w), 515 (s), 422 (w). NMR ( $\text{CDCl}_3$ ):  $^1\text{H}$   $\delta$  8.11 (dm,  $J_{\text{HP}} = 13.7$  Hz, 4H), 7.77–7.62 (m, 12H), 7.39 (t,  $^3J_{\text{HH}} = 7.7$  Hz, 1H), 7.15 (dd,  $^3J_{\text{HH}} = 7.7$  Hz,  $^4J_{\text{HH}} = 1.7$  Hz, 1H), 7.14 (dd,  $^3J_{\text{HH}} = 7.7$  Hz,  $^4J_{\text{HH}} = 1.7$  Hz, 1H), 3.82 (d,  $^3J_{\text{HP}} = 14.5$  Hz, 4H).  $^{13}\text{C}\{^1\text{H}\}$   $\delta$  151.6 (d,  $^2J_{\text{CP}} = 8.5$  Hz, py), 137.3, 134.8 (d,  $J_{\text{CP}} = 8.2$  Hz) (py), 132.4, 132.0 (d,  $^1J_{\text{CP}} = 93$  Hz), 131.5 ( $J_{\text{CP}} = 11.5$  Hz), 126.8 (py), 126.3 (q,  $^1J_{\text{CF}} = 208$  Hz,  $\text{CF}_3$ ), 42.0 (d,  $^1J_{\text{CP}} = 68.5$  Hz).  $^{31}\text{P}\{^1\text{H}\}$ :  $\delta$  30.8. Mass spectrum (ESI):  $[\text{M}+\text{H}]^+$  780.1059,  $[\text{M}+\text{Na}]^+$  802.0915. Anal. calcd for  $\text{C}_{35}\text{H}_{23}\text{NO}_2\text{F}_{12}\text{P}_2$ : C, 53.93; H, 2.97; N, 1.80. Found: C, 53.55; H, 3.27; N, 1.71.

**2,6-Bis[bis-3,5-bis((trifluoromethyl)phenyl)phosphinoylmethyl]pyridine (1b).** A solution of 3,5-bis(trifluoromethyl)bromobenzene (12.3 mL, 42.0 mmol) in dry THF (42 mL) was combined dropwise with a suspension of magnesium (1.0 g, 42.0 mmol) in dry THF (10 mL). The temperature rose during the addition, and the mixture was stirred (1 h). The resulting mixture was cooled (23 °C), and a solution of diethylphosphite (1.45 mL, 11.0 mmol) in dry THF (20 mL) was added dropwise. The mixture was refluxed (1 h) and then cooled (23 °C). A solution of 2,6-bis(chloromethyl)-pyridine (1.0 g, 5.7 mmol) in dry THF (20 mL) was added dropwise, and the mixture refluxed (12 h). The cooled mixture was quenched with a saturated aqueous solution of  $\text{NH}_4\text{Cl}$  (100 mL), and the aqueous phase separated from the organic phase. The aqueous phase was extracted with  $\text{CH}_2\text{Cl}_2$  ( $3 \times 20$  mL), and the combined organic phases were dried over  $\text{Na}_2\text{SO}_4$  and concentrated. The residue was crystallized from methanol giving a yellow brown powder, **1b**: yield: 1.77 g, 35%. Slow evaporation of the solvent provided a

- (15) Horwitz, E. P.; Muscatello, A. C.; Kalina, D. G.; Kaplan, L. *Sep. Sci. Technol.* **1981**, 16, 417.
- (16) Horwitz, E. P.; Kalina, D. G.; Muscatello, A. C. *Sep. Sci. Technol.* **1981**, 16, 403.
- (17) Romanovskiy, V. N.; Smirnov, I. V.; Babain, V. A.; Todd, T. A.; Herbst, R. S.; Law, J. D.; Brewer, K. N. *Solv. Extr. Ion Exch.* **2001**, 19, 1.
- (18) Law, J. D.; Herbst, R. S.; Todd, T. A.; Romanovskiy, V. N.; Babain, V. A.; Esimantovskiy, V. M.; Smirnov, I. V.; Zaitsev, B. N. *Solv. Extr. Ion Exch.* **2001**, 19, 23.
- (19) Herbst, R. S.; Law, J. D.; Todd, T. A.; Romanovskiy, V. N.; Babain, V. A.; Esimantovskiy, V. M.; Smirnov, I. V.; Zaitsev, B. N. *Solv. Extr. Ion Exch.* **2002**, 20, 429.
- (20) Romanovskiy, V. N.; Babain, V. A.; Alyapyshev, M. Yu.; Smirnov, I. V.; Herbst, R. S.; Law, J. D.; Todd, T. A. *Sep. Sci. Technol.* **2006**, 41, 2111.

- (21) Rezzonico, B.; Grigon-Dubois, M. *J. Chem. Res.* **1944**, 142.

second crop of crystals of **1b**: total yield 3.77 g, 63%; mp 228–230 °C. IR (KBr,  $\text{cm}^{-1}$ ): 3079 (w), 3036 (w), 2967 (w), 2921 (w), 1845 (w), 1619 (s), 1586 (s), 1457 (s), 1369 (vs), 1284 (vs), 1189 (vs), 1134 (vs), 990 (w), 906 (s), 844 (s), 762 (vw), 742 (w), 692 (s), 648 (vw), 611 (s), 520 (s), 486 (s). NMR ( $\text{CDCl}_3$ ):  $^1\text{H}$   $\delta$  8.30 (d,  $^3J_{\text{HP}} = 11.2$  Hz, 8H), 8.03 (s, 4H), 7.52 (t,  $^3J_{\text{HH}} = 7.7$  Hz, 1H), 7.22 (dd,  $^3J_{\text{HH}} = 7.7$  Hz,  $^4J_{\text{HH}} = 2.0$  Hz, 1H), 7.20 (dd,  $^3J_{\text{HH}} = 7.7$  Hz,  $^4J_{\text{HH}} = 2.0$  Hz, 1H), 3.80 (d,  $^2J_{\text{HP}} = 18.1$  Hz, 4H).  $^{13}\text{C}\{^1\text{H}\}$   $\delta$  151.0 (d,  $^2J_{\text{CP}} = 11$  Hz, py), 138.9 (py), 134.7 (d,  $^1J_{\text{CP}} = 99.0$  Hz), 133.0 (dq,  $^2J_{\text{CF}} = 34$  Hz,  $^3J_{\text{CP}} = 12$  Hz), 131.8 (d,  $^2J_{\text{CP}} = 12$  Hz), 126.8, 124.7 (py), 123.1 ( $^1J_{\text{CF}} = 270$  Hz,  $\text{CF}_3$ ), 40.0 (d,  $^1J_{\text{CP}} = 65.8$  Hz).  $^{31}\text{P}\{^1\text{H}\}$ :  $\delta$  26.3. Mass spectrum (ESI):  $[\text{M}+\text{H}]^+$  1052.0435,  $[\text{M}+\text{Na}]^+$  1074.0393. Anal. Calcd for  $\text{C}_{39}\text{H}_{19}\text{NO}_2\text{F}_{24}\text{P}_2$ : C, 44.55; H, 1.82; N, 1.33. Found: C, 43.72; H, 1.77; N, 1.38.

**Ligand Oxidations.** A sample of **1a** or **1b** (1 equiv) was dissolved in  $\text{CH}_2\text{Cl}_2$  and combined with *m*-chloroperbenzoic acid (77%, 1.3 equiv). The mixture was stirred and refluxed (12 h). The resulting mixture was quenched with saturated aqueous  $\text{NaHCO}_3$  (30 mL). The aqueous phase was extracted with  $\text{CH}_2\text{Cl}_2$  ( $3 \times 20$  mL). Organic phases were combined, dried with  $\text{Na}_2\text{SO}_4$  or  $\text{MgSO}_4$ , and concentrated.

**2,6-Bis[bis(2-(trifluoromethyl)phenyl)phosphinoylmethyl]pyridine N-Oxide (2a).** A white powder **2a** was obtained by crystallization from methanol: yield 0.79 g, 78%; mp: 118–120 °C. IR (KBr,  $\text{cm}^{-1}$ ): 3074 (w), 1569 (w), 1488 (w), 1428 (s), 1315 (vs), 1260 (s), 1179 (vs), 1118 (vs), 1035 (vs), 968 (s), 895 (w), 860 (w), 822 (w), 774 (vs), 710 (s), 639 (w), 592 (w), 518 (s), 489 (s). NMR ( $\text{CDCl}_3$ ):  $^1\text{H}$   $\delta$  8.10 (dm,  $J_{\text{HP}} = 14.3$  Hz, 4H), 7.70 (m, 4H), 7.60 (m, 10H), 7.05 (t,  $^3J_{\text{HH}} = 8.7$  Hz, 1H), 4.20 (d,  $^3J_{\text{HH}} = 13.8$  Hz, 4H).  $^{13}\text{C}\{^1\text{H}\}$   $\delta$  143.0 (d,  $^2J_{\text{CP}} = 13$  Hz, py), 133.0 (d,  $J_{\text{CP}} = 9.1$  Hz), 131.9, 131.4 (d,  $^1J_{\text{CP}} = 95$  Hz), 131.3 (d,  $J_{\text{CP}} = 11.8$  Hz), 127.5 (m), 125.6 (q,  $^1J_{\text{CF}} = 193$  Hz,  $\text{CF}_3$ ), 125.5 (py) 33.3 (d,  $^2J_{\text{CP}} = 72.8$  Hz).  $^{31}\text{P}\{^1\text{H}\}$ :  $\delta$  32.1. Mass spectrum (ESI)  $[\text{M}+\text{H}]^+$  796.0980,  $[\text{M}+\text{Na}]^+$  810.0844. Anal. Calcd for  $\text{C}_{35}\text{H}_{23}\text{NO}_3\text{F}_{12}\text{P}_2$ : C, 52.85; H, 2.91; N, 1.76. Found: C, 52.17; H, 3.37; N, 1.60.

**2,6-Bis[bis(3,5-bis(trifluoromethyl)phenyl)phosphinoylmethyl]pyridine N-Oxide (2b).** A white powder **2b** was obtained by crystallization from methanol: yield 0.76 g, 75%. A white cotton was obtained from acetone: yield 0.71 g, 70%. Suitable single crystals were obtained from a mixture of acetone and methanol: mp 235–240 °C. IR (KBr,  $\text{cm}^{-1}$ ): 3086 (vw), 2964 (vw), 2921 (s), 1575 (w), 1454 (w), 1415 (w), 1367 (s), 1283 (vs), 1189 (vs), 1136 (vs), 908 (s), 839 (s), 796 (w), 710 (s), 692 (s), 613 (w), 517 (s), 489 (s). NMR ( $\text{CDCl}_3$ ):  $^1\text{H}$   $\delta$  8.40 (d,  $^3J_{\text{HP}} = 11.8$  Hz, 8H), 8.05 (s, 4H), 7.43 (dd,  $^3J_{\text{HH}} = 7.7$  Hz,  $^4J_{\text{HH}} = 2$  Hz, 1H), 7.41 (dd,  $^3J_{\text{HH}} = 7.7$  Hz,  $^4J_{\text{HH}} = 2$  Hz, 1H), 7.15 (t,  $^3J_{\text{HH}} = 7.5$  Hz, 1H), 4.00 (d,  $^2J_{\text{CP}} = 15.2$  Hz, 4H).  $^{13}\text{C}\{^1\text{H}\}$   $\delta$  142.7 (d,  $^2J_{\text{CP}} = 10.7$  Hz, py), 134.0 (d,  $^1J_{\text{CP}} = 100$  Hz), 132.4 (dq,  $^2J_{\text{CF}} = 34$  Hz),  $^3J_{\text{CP}} = 13$  Hz), 131.7 (py), 131.1 (d,  $^2J_{\text{CP}} = 10$  Hz), 126.6 (m), 126.0 (py), 122.6 (q,  $^1J_{\text{CF}} = 273$  Hz,  $\text{CF}_3$ ) 34.7 (d,  $^1J_{\text{CP}} = 68.1$  Hz).  $^{31}\text{P}\{^1\text{H}\}$ :  $\delta$  27.9. Mass spectrum (ESI)  $[\text{M}+\text{H}]^+$  1068.0607,  $[\text{M}+\text{Na}]^+$  1090.0330. Anal. Calcd for  $\text{C}_{39}\text{H}_{19}\text{NO}_3\text{F}_{24}\text{P}_2$ : C, 43.88; H, 1.79; N, 1.31. Found: C, 43.20; H, 1.95; N, 1.30.

**Synthesis of Complexes. Nd(2a)(NO<sub>3</sub>)<sub>3</sub>.** A sample of **2a** (0.10 g, 0.13 mmol) was dissolved in acetone (5 mL) and combined with a solution of Nd(NO<sub>3</sub>)<sub>3</sub>·5H<sub>2</sub>O (0.055 g, 0.13 mmol) in MeOH (3 mL). The solution was stirred (12 h) and a white powder was recovered by filtration. Violet crystals suitable for X-ray analyses were obtained by recrystallization from a mixture of methanol, acetonitrile and acetone with slow evaporation (5 days): yield 0.072 g, 49%; mp: >250 °C. IR (KBr,  $\text{cm}^{-1}$ ): 3448 (w, br), 3163 (w), 3079 (s), 3005 (s), 2932 (s), 2854 (w), 2620 (w), 2572 (w), 2515 (m), 2445 (m), 2357 (m), 2304 (m), 2235 (w), 2158 (w), 2092 (w),

2048 (w), 1978 (m), 1855 (w), 1735 (s), 1582 (s), 1494 (vs), 1312 (vs), 1260 (s), 1179 (vs), 1119 (vs, br), 1031 (s), 970 (s), 892 (sh, s), 856 (s), 820 (s), 724 (s), 637 (s), 589 (s), 569 (sh, s), 505 (s).

**Nd(2a)(NO<sub>3</sub>)<sub>3</sub>·(CH<sub>3</sub>CN)<sub>0.5</sub>.** A sample of **2a** (0.2 g, 0.25 mmol) was dissolved in acetone (5 mL) and combined and stirred with a solution of Nd(NO<sub>3</sub>)<sub>3</sub>·5H<sub>2</sub>O (0.055 g, 0.126 mmol) in MeOH (3 mL). A white powder was recovered by filtration after 12 h. Violet crystals, suitable for X-ray analysis, were obtained by recrystallization from acetonitrile.

**Eu(2a)(NO<sub>3</sub>)<sub>3</sub>.** A sample of **2a** (0.5 g, 0.6 mmol) was dissolved in MeOH (5 mL) and combined with Eu(NO<sub>3</sub>)<sub>3</sub>·5H<sub>2</sub>O (0.269 g, 0.5 mmol) in MeOH (5 mL). A white precipitate formed after 1 h. The solid was recovered by filtration. It is insoluble in MeOH and partially soluble in  $\text{CH}_2\text{Cl}_2$  and DMF. Recrystallization from DMF slowly produced small crystals. IR: (KBr,  $\text{cm}^{-1}$ ): 3160 (w), 3080 (m), 3008 (m), 2940 (m), 2519 (w), 2448 (w), 2306 (w), 1730 (w), 1581 (m), 1494 (vs), 1435 (s), 1313 (vs), 1275 (m, sh), 1230 (m, sh), 1167 (vs), 1120 (vs), 1033 (s), 969 (w), 858 (m), 820 (m), 771 (s), 726 (s), 688 (w), 639 (w), 591 (w), 569 (w), 512 (s).

**Nd(2b)(NO<sub>3</sub>)<sub>3</sub>·(H<sub>2</sub>O)<sub>1.25</sub>.** A sample of **2b** (0.12 g, 0.09 mmol) was dissolved in acetone (5 mL) and combined with a solution of Nd(NO<sub>3</sub>)<sub>3</sub>·5H<sub>2</sub>O (0.04 g, 0.09 mmol) in acetone (3 mL). The mixture was stirred at 23 °C (12 h). A white powder was recovered after slow evaporation (7 d). Single crystals were obtained after recrystallization from hot dichloromethane and slow evaporation: mp: 200 °C (decomposed). IR (KBr,  $\text{cm}^{-1}$ ): 3449 (w, br), 3271 (vw), 3254 (vw), 3139 (w), 3093 (sh, w), 2929 (w, br), 2855 (w), 2769 (vw), 2674 (vw), 2524 (vw), 1944 (vw), 1847 (w), 1737 (w), 1620 (w), 1577 (w), 1495 (s), 1368 (s), 1284 (vs), 1184 (s), 1136 (vw), 1031 (w), 970 (w), 909 (w), 860 (w), 838 (w), 750 (w), 709 (sh, s), 690 (s), 641 (w), 613 (w), 569 (w), 514 (w).

**X-ray Diffraction Analyses.** Crystals of the ligands and complexes were placed in glass capillaries and mounted on a Bruker X8 Apex2 CCD-based X-ray diffractometer outfitted with an Oxford Cryostream 700 low temperature device and a normal focus Mo-target X-ray tube ( $\lambda = 0.71073\text{\AA}$ ) operated at 1500 W (50 kV, 30 mA). The data frames were integrated with the Bruker SAINT software package and processed with SADABS. The structures were solved and refined with the Bruker SHELXTL software package.<sup>22</sup> Lattice and data collection parameters are summarized in Table 1. Individual comments on each structure follow. **1a** and **2a**·MeOH: The structure solutions and refinements were well behaved. Non-hydrogen atoms were refined anisotropically, and H-atoms were included and refined in ideal positions with fixed  $U_{\text{iso}} = 1.2U_{\text{eq}}$  of C. **1b**·CH<sub>3</sub>OH: All non-hydrogen atoms were refined anisotropically and hydrogen atoms were placed in idealized positions and refined with fixed  $U_{\text{iso}} = 1.5U_{\text{eq}}$  of C and O of the MeOH-[O3, C40]. There are eight CF<sub>3</sub> groups on the molecule and a MeOH in the lattice and all are disordered. The treatment of the disorder is fully described in the Supporting Information. **2b**·(CH<sub>3</sub>)<sub>2</sub>CO: All non-hydrogen atoms were refined anisotropically. Hydrogen atoms were included in idealized portions and refined with  $U_{\text{iso}} = 1.2U_{\text{eq}}$  of C. The eight CF<sub>3</sub> groups and the acetone have large  $U_{\text{iso}}$  values and they are disordered. The disorder treatment is described in the Supporting Information. **Nd(2a)(NO<sub>3</sub>)<sub>3</sub>**: All non-hydrogen atoms were refined anisotropically. The hydrogen atoms on C were included in idealized positions and refined with  $U_{\text{iso}} = 1.2U_{\text{eq}}$  of the parent atom. There is disorder of the F-atom positions on C14. The treatment of the disorder is described in the Supporting Information.

(22) The crystallographic software used in these structure determinations include: Sheldrick, G.M., SHELXTL, v. 6.14; Bruker Analytical X-ray Madison, WI, 2001; Sheldrick, G.M., SADABS, v. 2.10. Program for Empirical Absorption Correction of Area Detector Data, University of Göttingen:Göttingen, Germany, 2003; SAINTPlus, v. 7.01, Bruker Analytical X-ray, Madison, WI, 2003.



Table 1. Crystallographic Data

	1a	2a•CH <sub>3</sub> OH	1b•CH <sub>3</sub> OH	2b•(CH <sub>3</sub> ) <sub>2</sub> CO
empirical formula	C <sub>35</sub> H <sub>23</sub> F <sub>12</sub> N <sub>2</sub> O <sub>2</sub> P <sub>2</sub>	C <sub>36</sub> H <sub>27</sub> F <sub>12</sub> N <sub>4</sub> O <sub>4</sub> P <sub>2</sub>	C <sub>40</sub> H <sub>23</sub> F <sub>24</sub> N <sub>2</sub> O <sub>3</sub> P <sub>2</sub>	C <sub>42</sub> H <sub>25</sub> F <sub>24</sub> N <sub>4</sub> O <sub>4</sub> P <sub>2</sub>
formula weight,	779.48	827.53	1083.53	1125.57
color, cryst. size (mm)	colorless, 0.52 × 0.52 × 0.27	colorless, 0.44 × 0.41 × 0.28	colorless, 0.41 × 0.08 × 0.08	colorless, 0.39 × 0.32 × 0.28
crystal system	monoclinic	triclinic	triclinic	triclinic
space group	<i>P</i> 2(1)/ <i>n</i>	<i>P</i> 1̄	<i>P</i> 1̄	<i>P</i> 1̄
<i>a</i> (Å)	18.0813(19)	8.5721(6)	12.1654(5)	12.1283(8)
<i>b</i> (Å)	9.4524(10)	13.1785(10)	12.5478(5)	12.5924(8)
<i>c</i> (Å)	19.956(2)	16.8087(13)	15.3684(7)	15.3841(10)
α (deg)	90	71.228(4)	83.752(2)	97.640(3)
β (deg)	103.949(5)	83.435(4)	88.970(2)	92.001(4)
γ (deg)	90	77.558(4)	87.809(2)	90.857(3)
<i>V</i> (Å <sup>3</sup> )	3310.1(6)	1753.5(2)	2330.11(17)	2326.8(2)
<i>Z</i>	4	2	2	2
<i>T</i> , (K)	228	228	228	225
μ (mm <sup>-1</sup> )	0.234	0.230	0.227	0.232
<i>D</i> <sub>calcd</sub> (gcm <sup>-3</sup> )	1.564	1.567	1.544	1.607
<i>F</i> <sub>ooo</sub>	1576	840	1080	1124
no. of reflections	88321	55811	53409	54230
no. independent reflections ( <i>R</i> <sub>int</sub> )	11136 (0.0261)	13145 (0.0202)	14291 (0.0366)	11537 (0.0191)
max/min transmission	0.93/0.88	0.939/0.906	0.980/0.910	0.93/0.91
final <i>R</i> <sub>1</sub> <sup>a</sup> , <i>wR</i> <sub>2</sub> <sup>b</sup> [ <i>I</i> > 2σ( <i>I</i> )]	0.0389, 0.0981	0.0538, 0.1428	0.0772, 0.2204	0.0809, 0.2343
<i>R</i> <sub>1</sub> , <i>wR</i> <sub>2</sub> (all data)	0.0653, 0.1224	0.0688, 0.1582	0.1292, 0.2591	0.0941, 0.2541
	Nd(2a)(NO <sub>3</sub> ) <sub>3</sub>	Nd(2a)(NO <sub>3</sub> ) <sub>3</sub> •(CH <sub>3</sub> CN) <sub>0.5</sub>	Eu(2a)(NO <sub>3</sub> ) <sub>3</sub>	Nd(2b)(NO <sub>3</sub> ) <sub>3</sub> •(H <sub>2</sub> O) <sub>1.25</sub>
empirical formula	C <sub>35</sub> H <sub>23</sub> F <sub>12</sub> N <sub>4</sub> NdO <sub>12</sub> P <sub>2</sub>	C <sub>36</sub> H <sub>24.5</sub> F <sub>12</sub> N <sub>4.5</sub> NdO <sub>12</sub> P <sub>2</sub>	C <sub>35</sub> H <sub>23</sub> EuF <sub>12</sub> N <sub>4</sub> O <sub>12</sub> P <sub>2</sub>	C <sub>39</sub> H <sub>21.5</sub> F <sub>24</sub> N <sub>4</sub> NdO <sub>13.25</sub> P <sub>2</sub>
formula weight,	1125.75	1146.28	1133.47	1420.28
color, cryst. size (mm)	lilac, 0.28 × 0.25 × 0.10	lilac, 0.25 × 0.20 × 0.13	colorless, 0.18 × 0.16 × 0.07	colorless, 0.35 × 0.23 × 0.17
crystal system	orthorhombic	monoclinic	orthorhombic	triclinic
space group	<i>P</i> 2(1)2(1)2(1)	<i>P</i> 2(1)/ <i>c</i>	<i>P</i> 2(1)2(1)2(1)	<i>P</i> 1̄
<i>a</i> (Å)	10.1697(4)	11.9160(6)	10.1129(5)	11.0642(6)
<i>b</i> (Å)	18.9472(7)	23.4118(11)	18.8663(10)	15.0247(8)
<i>c</i> (Å)	21.0152(8)	15.6768(7)	21.1388(10)	16.2086(9)
α (deg)	90	90	90	87.033(3)
β (deg)	90	94.698(4)	90	79.624(2)
γ (deg)	90	90	90	75.122(3)
<i>V</i> (Å <sup>3</sup> )	4049.4(3)	43587.7(4)	4033.1(3)	2561.5(2)
<i>Z</i>	4	4	4	2
<i>T</i> , (K)	225	225	228	225
μ (mm <sup>-1</sup> )	1.484	1.381	1.758	1.228
<i>D</i> <sub>calcd</sub> (gcm <sup>-3</sup> )	1.847	1.747	1.867	1.841
<i>F</i> <sub>ooo</sub>	2220	2264	2232	1391
no. of reflections	124872	101819	128628	81790
no. independent reflections ( <i>R</i> <sub>int</sub> )	15578 (0.0422)	13350 (0.1189)	15577 (0.0860)	19848 (0.0201)
max/min transmission	0.86/0.68	0.83/0.708	0.888/0.738	0.810/0.699
final <i>R</i> <sub>1</sub> <sup>a</sup> , <i>wR</i> <sub>2</sub> <sup>b</sup> [ <i>I</i> > 2σ( <i>I</i> )]	0.0369, 0.0805	0.0586, 0.1218	0.0410, 0.0819	0.0325, 0.0811
<i>R</i> <sub>1</sub> , <i>wR</i> <sub>2</sub> (all data)	0.0534, 0.0873	0.1202, 0.1456	0.0649, 0.0898	0.0407, 0.0899

$$^a R_1 = \sum |F_o| - |F_c| / \sum |F_o|, ^b wR_2 = \{ \sum [w(F_o^2 - F_c^2)^2] / \sum w(F_o^2)^2 \}^{1/2}.$$

**Nd(2a)(NO<sub>3</sub>)<sub>3</sub>•(CH<sub>3</sub>CN)<sub>0.5</sub>:** All non-hydrogen atoms were refined anisotropically. The hydrogen atoms of **2a** were placed in ideal positions and refined with  $U_{iso} = 1.2U_{eq}$  of the parent atom. There is a partially occupied CH<sub>3</sub>CN solvent molecule, and its H-atoms were placed in ideal positions and refined with  $U_{iso} = 1.5U_{eq}$ . There is a small degree of disorder of the F-atoms on C28 and C35. **Eu(2a)(NO<sub>3</sub>)<sub>3</sub>:** All non-hydrogen atoms except disordered F-atoms on C<sub>30</sub> were refined anisotropically. The H-atoms on C were placed in ideal positions and refined with  $U_{iso} = 1.2U_{eq}$  of the parent atom. The treatment of the F-atom disorder is described in the Supporting Information. **Nd(2b)(NO<sub>3</sub>)<sub>3</sub>•(H<sub>2</sub>O)<sub>1.25</sub>:** There are two Nd(2b)(NO<sub>3</sub>)<sub>3</sub> complexes and 2.5 molecules of water per unit cell. All non-hydrogen atoms were refined anisotropically. The H-atoms on C were placed in ideal positions and refined with  $U_{iso} = 1.2U_{eq}$ . There are three disordered CF<sub>3</sub> groups (C14, C21, C28) and their treatment is described in Supporting Information. Selected bond distances for the ligands and the complexes are summarized in Table 2.

**Computational Analyses.** Geometry optimization of ground-state structures and corresponding vibrational frequencies were

carried out with the Gaussian 03 suite of programs.<sup>23</sup> Analytic calculations of the energy Hessian confirmed that minimum energy structures had no imaginary frequencies. Given that Pople type triple-ζ are adequate for phosphorus atoms,<sup>24</sup> all calculations were

- (23) Frisch, M. J.; Trucks, G. W.; Schlegel, H. B.; Scuseria, G. E.; Robb, M.; Cheeseman, J. R.; Montgomery, J. A.; Vreven, J. A.; Kudin, K. N.; Burant, J. C.; Millam, J. M.; Iyengar, S. S.; Tomasi, J.; Barone, V.; Mennucci, B.; Cossi, M.; Scalmani, G.; Rega, N.; Petersson, G. A.; Nakatsuji, H.; Hada, M.; Ehara, M.; Toyota, K.; Fukuda, R.; Hasegawa, J.; Ishida, M.; Nakajima, T.; Honda, Y.; Kitao, O.; Nakai, H.; Klene, M.; Li, X.; Knox, J. E.; Hratchian, H. P.; Cross, J. B.; Adamo, C.; Jaramillo, J.; Gomperts, R.; Stratmann, R. E.; Yazyev, O.; Austin, A. J.; Cammi, R.; Pomelli, C.; Ochterski, J. W.; Ayala, P. Y.; Morokuma, K.; Voth, G. A.; Salvador, P.; Dannenberg, J. J.; Zakrzewski, V. G.; Dapprich, S.; Daniels, A. D.; Strain, M. C.; Farkas, O.; Malick, D. K.; Rabuck, A. D.; Raghavachari, K.; Foresman, J. B.; Ortiz, J. V.; Cui, Q.; Baboul, A. G.; Clifford, S.; Cioslowski, J.; Stefanov, B. B.; Liu, G.; Liashenko, A.; Piskorz, P.; Komaromi, I.; Martin, R. L.; Fox, D. J.; Keith, T.; Al-Laham, M. A.; Peng, C. Y.; Nanayakkara, A.; Challacombe, M.; Gill, P. M. W.; Johnson, B.; Chen, W.; Wong, M. W.; Gonzalez, C.; Pople, G. A., *Gaussian 03*, Revision C.02; Gaussian, Inc.: Wallingford, CT, 2004.

Table 2. Selected Bond Lengths (Å)

bond	1a	2a•CH <sub>3</sub> OH	1b•CH <sub>3</sub> OH	2b•(CH <sub>3</sub> ) <sub>2</sub> CO	Nd(2a)(NO <sub>3</sub> ) <sub>3</sub>	Nd(2a)(NO <sub>3</sub> ) <sub>3</sub> •(CH <sub>3</sub> CN) <sub>0.5</sub>	Eu(2a)(NO <sub>3</sub> ) <sub>3</sub>	Nd(2b)(NO <sub>3</sub> ) <sub>3</sub> •(H <sub>2</sub> O) <sub>1.25</sub>
P=O	P(1)–O(1) 1.4815(11) P(2)–O(2) 1.4754(12)	P(1)–O(2) 1.4832(12) P(2)–O(3) 1.4816(13)	P(1)–O(1) 1.484(2) P(2)–O(2) 1.482(2)	P(1)–O(2) 1.478(2) P(2)–O(3) 1.482(2)	P(1)–O(2) 1.489(2) P(2)–O(3) 1.493(2)	P(1)–O(2) 1.495(4) P(2)–O(3) 1.500(3)	P(1)–O(2) 1.491(3) P(2)–O(3) 1.495(2)	P(1)–O(2) 1.5018(13) P(2)–O(3) 1.5039(14)
N–O		N(1)–O(1) 1.3003(18) P(1)–C(6) 1.8180(16)	N(1)–O(1) 1.288(3) P(1)–C(6) 1.798(3)	N(1)–O(1) 1.288(3) P(1)–C(6) 1.815(3)	N(1)–O(1) 1.329(3) P(1)–C(6) 1.828(3)	N(1)–O(1) 1.332(5) P(1)–C(6) 1.822(5)	N(1)–O(1) 1.328(3) P(1)–C(6) 1.807(3)	N(1)–O(1) 1.3300(18) P(1)–C(6) 1.8136(17)
P–C	P(2)–C(21) 1.8242(15)	P(2)–C(21) 1.8241(17)	P(2)–C(7) 1.803(3)	P(2)–C(23) 1.812(3)	P(2)–C(7) 1.810(3) Nd–O(1) 2.459(2)	P(2)–C(7) 1.822(5) Nd–O(1) 2.385(3)	P(2)–C(7) 1.823(3) Eu–O(1) 2.424(2)	P(2)–C(7) 1.818(2) Nd–O(1) 2.3741(12)
M–O <sub>lig</sub>					Nd–O(2) 2.362(2) Nd–O(3) 2.372(2)	Nd–O(2) 2.397(3) Nd–O(3) 2.425(3)	Eu–O(2) 2.334(2) Eu–O(3) 2.320(2)	Nd–O(2) 2.4567(13) Nd–O(3) 2.3956(13)
M–O <sub>nitrate</sub>					Nd–O(4) 2.503(3) Nd–O(5) 2.569(3)	Nd–O(4) 2.537(4) Nd–O(5) 2.537(4)	Eu–O(4) 2.561(3) Eu–O(5) 2.463(3)	Nd–O(4) 2.5357(14) Nd–O(5) 2.5348(16)
					Nd–O(7) 2.524(2) Nd–O(8) 2.539(2)	Nd–O(7) 2.516(4) Nd–O(8) 2.530(4)	Eu–O(7) 2.528(3) Eu–O(8) 2.490(3)	Nd–O(7) 2.5370(16) Nd–O(8) 2.5604(17)
					Nd–O(10) 2.565(3) Nd–O(11) 2.529(3)	Nd–O(10) 2.524(4) Nd–O(11) 2.514(4)	Eu–O(10) 2.481(3) Eu–O(11) 2.510(3)	Nd–O(10) 2.4998(18) Nd–O(11) 2.4732(17)

performed in the gas-phase with the B3YLP hybrid density functional<sup>25</sup> and 6-311G(d,p) and 6-311++G(d,p) Pople basis sets. On the basis of evaluation of the resulting vibrational frequency values produced for both basis sets for **2a** and several model compounds, that is, pyridine-1-oxide and triphenylphosphine oxide, the 6-311G(d,p) basis set offered the best balance between computational cost and frequency accuracy. The geometries and energies were not corrected for basis set superposition error (BSSE) since the larger basis sets combined with Density Functional Theory were expected to produce smaller errors.<sup>26</sup> The harmonic frequency algorithm employed by Gaussian 03 generates a set of atom motions for each frequency. The visualizer option in GaussView 3.0<sup>27</sup> was employed to identify the frequency values corresponding to  $\nu_{\text{PO}}$  and  $\nu_{\text{NO}}$ . The geometry optimized coordinates and frequencies for the compounds of interest to this paper can be found in the Supporting Information.

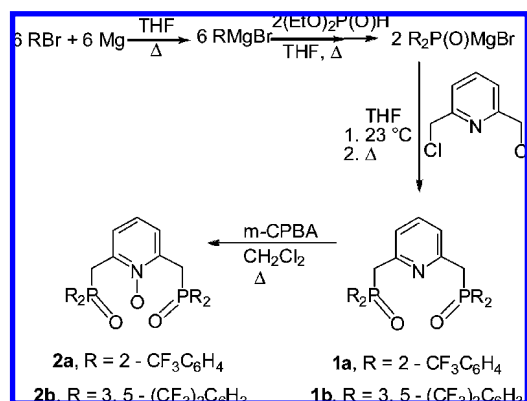
## Results and Discussion

As detailed in a prior report,<sup>3</sup> several symmetrical alkyl and aryl substituted NPOPO ligands can be prepared in good yields and purities by using traditional Arbusov or Michaelis–Becker reactions<sup>28,29</sup> on 2,6-bis(chloromethyl) pyridine. Subsequent N-oxidation of the NPOPO pyridine intermediates produces the desired NOPOPO ligands. In addition, we found that phosphinoyl Grignard reagents, in combination with 2,6-bis(chloromethyl) pyridine, provide facile entry to both symmetrical and asymmetrical alkyl and aryl NPOPO intermediates. This route is often preferred because of the relative efficiency of the one-pot formation and transformation of the Grignard reagents. In the present study, the intermediate aryl Grignard reagents, 2-CF<sub>3</sub>C<sub>6</sub>H<sub>4</sub>MgBr,<sup>30</sup> and 3,5-(CF<sub>3</sub>)<sub>2</sub>C<sub>6</sub>H<sub>3</sub>MgBr<sup>31</sup> were prepared in dry THF and mixed with (EtO)<sub>2</sub>P(O)H (~4:1). The respective phosphinoyl Grignard reagents [(2-CF<sub>3</sub>)C<sub>6</sub>H<sub>4</sub>]<sub>2</sub>P(O)MgBr and [3,5-(CF<sub>3</sub>)<sub>2</sub>C<sub>6</sub>H<sub>3</sub>]<sub>2</sub>P(O)MgBr were obtained in good yields and, without isolation, these were combined (2:1) with 2,6-bis(chloromethyl) pyridine. Work-up of the product mixture provided the NPOPO compounds {[ (2-CF<sub>3</sub>)C<sub>6</sub>H<sub>4</sub>]<sub>2</sub>P(O)CH<sub>2</sub> }<sub>2</sub>-C<sub>5</sub>H<sub>3</sub>N (**1a**) and {[ (3,5-(CF<sub>3</sub>)<sub>2</sub>C<sub>6</sub>H<sub>3</sub>]<sub>2</sub>P(O)CH<sub>2</sub> }<sub>2</sub>-C<sub>5</sub>H<sub>3</sub>N (**1b**), as solids, in good yields: 90% and 63%, respectively. Both intermediates were dissolved in CH<sub>2</sub>Cl<sub>2</sub> and N-oxidized with *m*-chloroperbenzoic acid. Following standard solution work-up, the target NOPOPO ligands {[ (2-CF<sub>3</sub>)C<sub>6</sub>H<sub>4</sub>]<sub>2</sub>P(O)CH<sub>2</sub> }<sub>2</sub>-C<sub>5</sub>H<sub>3</sub>NO (**2a**) and {[ (3,5-(CF<sub>3</sub>)<sub>2</sub>C<sub>6</sub>H<sub>3</sub>]<sub>2</sub>P(O)CH<sub>2</sub> }<sub>2</sub>-C<sub>5</sub>H<sub>3</sub>NO (**2b**) were isolated as white solids in 78% and 75% yields, respectively. The syntheses are summarized in Scheme 1.

Characterization data substantiate the proposed formulations of **1a**, **1b**, **2a**, and **2b**. Each compound displays a

- (24) McLean, A. D.; Chandler, G. S. *J. Chem. Phys.* **1980**, 72, 5639.
- (25) Sousa, S. P.; Fernandes, S. A.; Ramos, M. J. *J. Phys. Chem. A* **2007**, 111, 10439.
- (26) Zhano, Y.; Truhlar, D. G. *J. Chem. Theory Comput.* **2005**, 1, 415.
- (27) Dennington, Roy, II; Keith, Todd; Millam, John; Eppinnett, Ken; Hovell, W. Lee; and Gilliland, Ray; *GaussView*, Version 3.09; Semichem, Inc.: Shawnee Mission, KS, 2003.
- (28) Emsley, J.; Hall, D. *The Chemistry of Phosphorus*; Harper and Row: London, 1976.
- (29) Quin, L. D. *A Guide to Organophosphorus Chemistry*; Wiley-Interscience: New York, 2000.
- (30) McKinsty, L.; Livinghouse, T. *Tetrahedron* **1994**, 50, 6145.
- (31) Casalnuovo, A. L.; RajanBabu, T. V.; Ayers, T. A.; Warren, T. H. *J. Am. Chem. Soc.* **1994**, 116, 9869.

Scheme 1



satisfactory CHN elemental analysis, and intense  $[M+H]^+$  and  $[M+Na]^+$  ions in the high resolution ESI-MS are observed. In prior infrared analyses of alkyl and aryl substituted NPOPO and NOPOPO ligands,<sup>1–6</sup> despite a crowded fingerprint region  $1700\text{--}700\text{ cm}^{-1}$ , we have generally succeeded in making tentative frequency assignments in the regions  $1200\text{--}1150$  and  $1290\text{--}1230\text{ cm}^{-1}$  to  $P=O$  and  $N\text{--}O$  stretching modes, respectively. However, because of the numerous  $CF_3$  stretching and bending modes in **1a,b** and **2a,b**, the fingerprint region is even more complex in comparison to the parent aryl NPOPO,  $[Ph_2P(O)CH_2]_2C_5H_3N$  (**1c**) and NOPOPO,  $[Ph_2P(O)CH_2]_2C_5H_3NO$  (**2c**). This has made assignments of the  $\nu_{PO}$  and  $\nu_{NO}$  stretching modes in the  $CF_3$  decorated ligands less certain. Nonetheless, the experimental  $\nu_{PO}$  stretch has been assigned to strong bands centered at  $1179$  (**1a**) and  $1189\text{ cm}^{-1}$  (**1b**). These values compare favorably with the  $\nu_{PO}$  band assigned in **1c**,<sup>2</sup>  $1195\text{ cm}^{-1}$ . As expected, no strong band is observed in the  $N\text{--}O$  stretching region  $1290\text{--}1230\text{ cm}^{-1}$ . Following N-oxidation, the phosphoryl stretching frequencies in **2a** and **2b** remain unchanged from those observed for their pyridine progenitors. This is similar to the observations found for the conversion of **1c** to **2c**. In that case, the  $\nu_{PO}$  frequency in **2c** is slightly lower,  $1188\text{ cm}^{-1}$ , than in **1c**. In addition, **2a** and **2b** display additional strong bands at  $1260$  and  $1283\text{ cm}^{-1}$ , respectively, and these are tentatively assigned to the  $\nu_{NO}$  mode. These appear at higher frequency than the  $\nu_{NO}$  band for **2c**,<sup>2</sup>  $1235\text{ cm}^{-1}$ . The up-frequency shifts may result from increased group electronegativities for the  $CF_3$  decorated  $[(CF_3)_2C_6H_3]_2P(O)CH_2$  and  $[(CF_3)_2C_6H_3]_2P(O)CH_2$  groups in **2a** and **2b**.

In an effort to provide additional support for the tentative  $\nu_{PO}$  and  $\nu_{NO}$  vibrational mode assignments made here and in our past studies,<sup>1–6</sup> Gaussian calculations were performed on several simple phosphine oxide fragments, as well as on **1a**, **1b**, **2a**, and **2b**. The computational and experimental data are summarized in Table 3. The computed values of  $\nu_{PO}$  for  $Ph_3PO$ ,  $Ph_2(Me)PO$ , and  $Ph_2(CF_3)PO$  fall within the region  $1240\text{--}1150\text{ cm}^{-1}$  typically ascribed to phosphine oxides with aryl substituent groups.<sup>28,32,33</sup> It might be expected that the calculated  $\nu_{PO}$  values would increase with increasing electron withdrawal on the P-atom resulting in an order  $Ph_2(Me)PO < Ph_3PO < Ph_2(CF_3)PO$ . The fact that the calculated  $\nu_{PO}$  for  $Ph_2(Me)PO$  falls in between the  $\nu_{PO}$  for the other two

Table 3. Gaussian Computation of  $P=O$  and  $N\text{--}O$  Stretching Frequencies

compound	vibrational mode	computed frequency ( $\text{cm}^{-1}$ )	experimental frequency ( $\text{cm}^{-1}$ )
<b>1a</b>	$\nu_{PO}$	1219 1222	1179
<b>1b</b>	$\nu_{PO}$	1207	1189
<b>1c</b>	$\nu_{PO}$	1200 1205	1195
<b>2a</b>	$\nu_{PO}$	1216 1225	1179
	$\nu_{NO}$	1281	1260
<b>2b</b>	$\nu_{PO}$	1201	1189
	$\nu_{NO}$	1267	1283
<b>2c</b>	$\nu_{PO}$	1197 1211	1188
	$\nu_{NO}$	1282 1313	1234
$Ph_3PO$	$\nu_{PO}$	1187	1205–1185 <sup>34,35</sup>
$Ph_2(Me)PO$	$\nu_{PO}$	1202	1202–1172 <sup>35,36</sup>
$Ph_2(CF_3)PO$	$\nu_{PO}$	1239	1226 <sup>37</sup>
pyrN-O	$\nu_{NO}$	1322	1340–1265 <sup>38,39</sup>

molecules may result from a secondary influence on the electron population in the  $P=O$  bond, or this may simply reflect the uncertainty in the computed values which is estimated to be  $\pm 30\text{ cm}^{-1}$ . The values computed for **1a**, **1b**, **2a**, and **2b** are all very similar to each other and to the model fragments. These observations support the  $\nu_{PO}$  band assignments given above. The computed  $\nu_{NO}$  frequencies for pyridine N-oxide,  $1322\text{ cm}^{-1}$ , **2a**,  $1281\text{ cm}^{-1}$ , and **2b**,  $1267\text{ cm}^{-1}$  are similar to each other. The differences may reflect electronic differences or they may once more mirror the larger computational error found with pyridine N-oxide derivatives ( $\pm 50\text{ cm}^{-1}$ ). It is well-known that experimental  $\nu_{NO}$  frequencies are sensitive to electronic effects exerted by ring substituents, as well as the phase of the sample used to record spectra.<sup>39,40</sup>

The  $^{31}P$  NMR spectra for **1a**, **1b**, **2a**, and **2b** each display a single resonance in the narrow chemical shift range  $\delta$   $33\text{--}26$  and, as observed previously,<sup>2,3</sup> the  $^{31}P$  resonance for each N-oxide is slightly (1–2 ppm) downfield of its pyridine progenitor. It is also noteworthy that the  $^{31}P$  chemical shifts in **1a** and **2a** are identical to the shifts recorded previously<sup>3</sup> for the tolyl analogues, and the shifts for **1b** and **2b** are  $\sim 4$  ppm *upfield* of the respective shifts in **1a** and **2a**. Hence, the 2- $CF_3$  substituents in **1a** and **2a** and the 3,5- $(CF_3)_2$  substituents in **1b** and **2b** apparently do not *dramatically* impact the electronic character of the  $P=O$  groups as assessed by  $^{31}P$  NMR. The  $^1H$  and  $^{13}C\{^1H\}$  NMR spectra are also comparable to the spectra observed for the phenyl and tolyl respective NOPO and NOPOPO analogues.<sup>2,3</sup>

To confirm the molecular structure of this class of ligands, the single crystal X-ray diffraction molecular structure determination for **1a** was undertaken. A view of the molecule is shown in Figure 1, and selected bond lengths are

(32) NIST Standard Reference Data Program Collection, Origin: Sadtler Research Laboratories under US-EPA contract.

(33) DeBolster, M. W. G.; Groeneveld, W. L. *Top. Phosphorus Chem.* **1976**, 8, 273.

(34) Gramstad, T. *Acta Chem. Scand.* **1992**, 46, 1087.

(35) An unattributed compendium found on the website at [www.bu.edu/gale/analyses/nuPO\\_Data\\_File/nuPO%20data%20](http://www.bu.edu/gale/analyses/nuPO_Data_File/nuPO%20data%20).

(36) Shvets, A. A.; Safaryan, G. P.; Shvets, S. A. *Russ. J. Gen. Chem.* **2000**, 70, 1037.



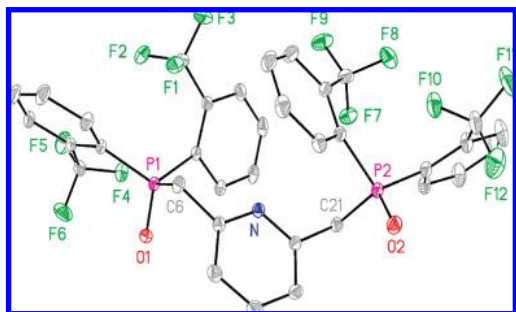


**Figure 1.** Molecular structure and atom labeling scheme for **1a** (20% thermal ellipsoids; all hydrogen atoms omitted for clarity).

summarized in Table 2. As expected, the molecule consists of a planar pyridine ring with pendent  $-\text{CH}_2\text{P}(\text{O})(2-\text{CF}_3\text{C}_6\text{H}_4)_2$  groups on the 2- and 6- positions. The  $\text{P}=\text{O}$  bond vectors are rotated away from the space occupied by the in-plane pyridine N-atom lone electron pair. This is illustrated by calculation of mean planes containing  $\text{P1O1C6}$  and  $\text{NC1-C2C3C4C5C6}$ ; the angle between these planes is  $86.7^\circ$ . This arrangement is anticipated based upon the structure reported for  $[\text{Ph}_2\text{P}(\text{O})\text{CH}_2]_2\text{C}_5\text{H}_3\text{N}$ , **1c**.<sup>41</sup> The average  $\text{P}=\text{O}$  bond length,  $1.478(1) \text{ \AA}$ , is comparable to the average value observed in **1c**,  $1.480(7) \text{ \AA}$ . However, an interesting unique feature appears in **1a** compared to **1c**: the non-bonded distances  $\text{F}(4)\cdots\text{P}(1)$   $2.883 \text{ \AA}$  and  $\text{F}(10)\cdots\text{P}(2)$   $2.932 \text{ \AA}$  are unusually short compared to the sum of van der Waals radii,  $3.27 \text{ \AA}$ .<sup>42</sup> In addition, the distances  $\text{F}(1)\cdots\text{P}(1)$ ,  $3.205 \text{ \AA}$ , and  $\text{F}(7)\cdots\text{P}(2)$ ,  $3.133 \text{ \AA}$ , are slightly shorter than expected. This feature, involving P(V) centers and aryl  $\text{CF}_3$  groups, has also recently been observed in  $(2-\text{CF}_3\text{C}_6\text{H}_5)_2\text{P}(\text{S})(\text{SH})$  where the related non-bonded distances are  $\text{F}\cdots\text{P}$   $2.968 \text{ \AA}$  and  $3.165 \text{ \AA}$ .<sup>43</sup> These suggest that weak electronic interactions exist between the electronegative F atoms and the backside of the P(V) center in both families of compounds. The geometry and bond angles about P(1) and P(2) further support this conclusion. Both P(1) and P(2) are tetrahedral with average angles  $109.5^\circ$  at P(1) and  $109.4^\circ$  at P(2). However, the tetrahedra are distorted, with larger  $\text{X}-\text{P}-\text{Y}$  angles facing the positions occupied by F(1), F(4), F(7), and F(10).<sup>44</sup>

The observation of short non-bonded  $\text{F}\cdots\text{P}$  interactions in **1a** led us to also determine the molecular structures of **1b**, **2a**, and **2b**. For molecule **1b** with  $\text{CF}_3$  groups at the 3- and 5- positions of the aryl rings (total of eight  $\text{CF}_3$  groups), all  $\text{CF}_3$  groups show large anisotropic thermal parameters, and four (on C(14), C(15), C(22), and C(31)) are disordered. In addition, the unit cell contains a disordered

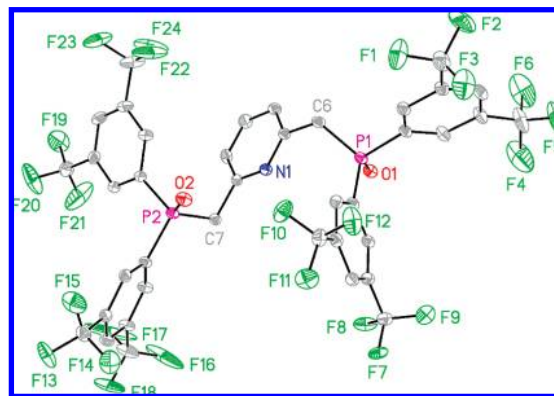


**Figure 2.** Molecular structure and atom labeling scheme for **1b**· $\text{CH}_3\text{OH}$  (20% thermal ellipsoids; all hydrogen atoms and disordered  $\text{CH}_3\text{OH}$  omitted for clarity).

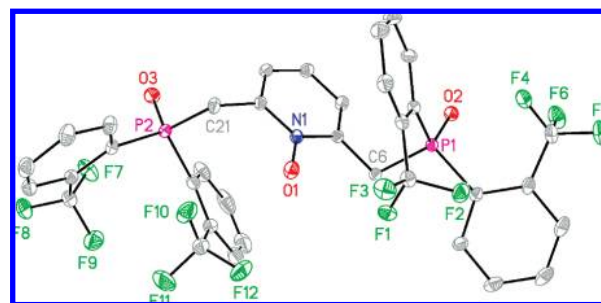


**Figure 3.** Molecular structure and atom labeling scheme for **2a**· $\text{CH}_3\text{OH}$  (20% thermal ellipsoids; all hydrogen atoms and  $\text{CH}_3\text{OH}$  omitted for clarity).

solvent molecule  $\text{CH}_3\text{OH}$ . These features obscure the analysis of the non-bonded  $\text{F}\cdots\text{P}$  distances, but it appears that none of the F-atoms makes close approach to the central P-atoms. The majority of  $\text{F}\cdots\text{P}$  distances exceed  $4.0 \text{ \AA}$  with the shortest  $\text{F}(16)\cdots\text{P}(1)$ ,  $3.55 \text{ \AA}$ , being significantly greater than the sum of van der Waals radii. This is expected as the 3- and 5- positions are well removed from the P-atom environment. A view of **1b** is shown in Figure 2 and selected bond lengths are presented in Table 2. The average  $\text{P}=\text{O}$  bond length in **1b**,  $1.483(1) \text{ \AA}$ , is comparable to that in **1a** and **1c**. The phosphorus atom geometries are both tetrahedral, and the bond angles show greater min/max variation than in **1a**:  $103.07^\circ$ – $114.55^\circ$ .

The N-oxidized derivative **2a**, contains a  $\text{CH}_3\text{OH}$  molecule in the unit cell, and all heavy-atom positions refined properly. Like in **2c**,<sup>2</sup> the  $\text{P}=\text{O}$  bond vectors are rotated away from the N–O bond vector. In this case the mean  $\text{P1O2C6}$  plane makes an angle of  $63.7^\circ$  with the mean  $\text{N1C1C2C3C4C5C6}$  plane. A view of the molecule without the  $\text{CH}_3\text{OH}$  solvent molecule appears in Figure 3, and selected bond distances are given in Table 2. The average  $\text{P}=\text{O}$  bond length,  $1.4824(13) \text{ \AA}$ , is essentially identical to the average values in **1a** and **2c**. Hence, as noted before, N-oxidation and  $\text{CF}_3$  substituted do not appear to significantly impact  $\text{P}=\text{O}$  bond lengths or  $\text{P}=\text{O}$  stretching frequencies (vide supra). The N–O bond length in **2a** is  $1.3003(18) \text{ \AA}$ , and this is slightly shorter than the value in **2c**,  $1.315(6) \text{ \AA}$ .<sup>2</sup> The question then becomes: does N-oxidation alter the  $\text{F}\cdots\text{P}$  non-bonded interactions between the 2- $\text{CF}_3$  substituents and the P-atoms? Examination of the environments around P(1) and P(2) in

(37) Lindner, E.; Kranz, H. *Z. Naturforsch. B.* **1967**, *22B*, 675.

(38) NIST Standard Reference Data Program Collection, Origin: Coblenz (No. 10231).

(39) Mielke, Z. *Spectrochim. Acta* **1983**, *34A*, 141.

(40) Herlocker, D. W.; Drago, R. S.; Meek, V. I. *Inorg. Chem.* **1966**, *5*, 2012.

(41) Szbyk, E.; Zhang, Z. Y.; Palenik, G. J.; Palenik, R. C.; Colgate, S. O. *Acta Crystallogr.* **1989**, *C45*, 1234.

(42) Boudi, J. *Phys. Chem.* **1964**, *68*, 441.

(43) Klaehn, J. R.; Peterman, D. R.; Harrup, M. K.; Tillotson, R. D.; Luther, T. A.; Law, J. D.; Daniels, L. M. *Inorg. Chim. Acta* **2008**, *361*, 2522.

(44) For example  $\text{F}(1)/\text{C}(7)-\text{P}(1)-\text{C}(14)$ ,  $112.65(6)^\circ$ ;  $\text{F}(4)/\text{O}(1)-\text{P}(1)-\text{C}(14)$ ,  $111.82(6)^\circ$ ;  $\text{F}(7)/\text{C}(22)-\text{P}(2)-\text{C}(29)$ ,  $113.61(7)^\circ$ ;  $\text{F}(10)/\text{O}(2)-\text{P}(2)-\text{C}(21)$ ,  $111.83(7)^\circ$ .

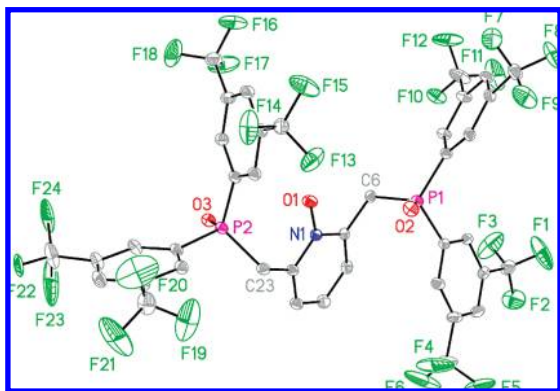


**Figure 4.** Molecular structure and atom labeling scheme for **2b**·(CH<sub>3</sub>)<sub>2</sub>CO (20% thermal ellipsoids; all hydrogen atoms and (CH<sub>3</sub>)<sub>2</sub>CO omitted for clarity).

**2a** show, once more, four interactions shorter than the sum of P and F van der Waals radii: F(1)···P(1), 3.117 Å, F(4)···P(1), 2.989 Å, F(7)···P(2), 2.945 Å, and F(10)···P(2), 2.980 Å. The solvent molecule CH<sub>3</sub>OH weakly hydrogen bonds with a neighboring phosphoryl O-atom.<sup>45</sup>

The molecular structure of **2b** is shown in Figure 4. The unit cell includes a molecule of acetone that is disordered over two positions, and this molecule is not shown in Figure 4. In addition, the CF<sub>3</sub> groups are disordered in a fashion similar to that found with its pyridine progenitor **1b**. None of the non-bonded F···P distances are shorter than 3.27 Å, and the two shortest distances, F(7)···P(2) and F(10)···P(2), are greater than 3.6 Å. The molecule shows its two P=O bond vectors rotated away from the N–O bond vector with the average P=O bond length 1.480(2) Å and N–O bond length 1.288(3) Å.

The observation that **2a** and **2b** are obtained in atom-efficient syntheses as easily purified solids that are soluble in the process solvent FS-13 (~0.01 M) makes them potentially attractive as liquid–liquid extraction reagents since the alternative hydrocarbon soluble extractant [(2-EtHx)<sub>2</sub>P(O)CH<sub>2</sub>]<sub>2</sub>C<sub>5</sub>H<sub>3</sub>NO is a heavy oil that must be purified with care. However, before embarking on time-consuming extraction analyses with actinide ions and fission product species, it is important to explore the coordination behavior of the new ligands and compare this against the coordination behavior of the related ligand, [Ph<sub>2</sub>P(O)CH<sub>2</sub>]<sub>2</sub>C<sub>5</sub>H<sub>3</sub>NO, **2c**, using Ln(NO<sub>3</sub>)<sub>3</sub> compounds as surrogates for trivalent actinides. Combining ratios **2a** or **2b** with the early lanthanides Nd(III) and Eu(III) L/Ln = 1:1, 2:1 and excess:1 were explored with several solvent combinations. On the basis of earlier studies with **2c** and related aryl and alkyl analogues,<sup>1,3</sup> it was expected that 2:1 complexes would form. However, in no case were the 2:1 complexes isolated and structurally characterized. Crystalline 1:1 complexes with Nd(III) and Eu(III) were obtained and selected features of four complexes are summarized.

**Nd(2a)(NO<sub>3</sub>)<sub>3</sub>.** The 1:1 combination of **2a** and Nd(NO<sub>3</sub>)<sub>3</sub> in a mixed acetone/MeOH solution led to the isolation of

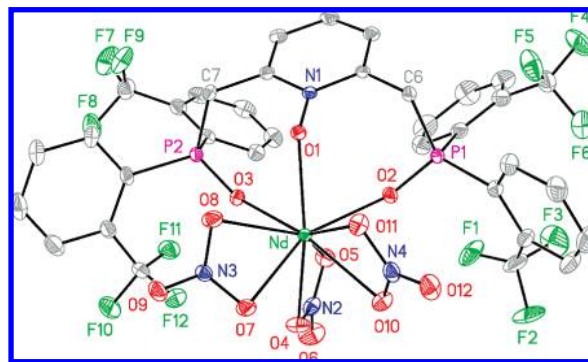


**Figure 5.** Molecular structure and atom labeling scheme for Nd(**2a**)(NO<sub>3</sub>)<sub>3</sub> (20% thermal ellipsoids; all hydrogen atoms omitted for clarity).

Nd(**2a**)(NO<sub>3</sub>)<sub>3</sub>. An infrared spectrum for the complex in KBr shows a strong band at 1119 cm<sup>-1</sup> that is tentatively assigned to a metal coordinated P=O stretch. This represents a 60 cm<sup>-1</sup> coordination shift from the free ligand consistent with a strong **2a**/Nd(III) interaction. Although the region 1340–1240 cm<sup>-1</sup> is rich in absorptions, a band at 1260 cm<sup>-1</sup> is tentatively assigned to coordinated pyridine N–O. A single crystal X-ray analysis for the complex, confirms that **2a** forms a 1:1 tridentate chelate complex with Nd(NO<sub>3</sub>)<sub>3</sub>, and a view of the molecule is shown in Figure 5. Selected bond lengths are presented in Table 2. The Nd(III) is coordinated to one tridentate ligand **2a** and three bidentate NO<sub>3</sub><sup>-</sup> resulting in a distorted nine-coordinate sphenoid polyhedron. One CF<sub>3</sub> (C(14)) is disordered over two positions, and the C(15)–C(20) ring is slightly irregular. The structural parameters can be compared against data for the complex Nd(**2c**)(NO<sub>3</sub>)<sub>3</sub>. The Nd–O(P) distances in the new complex, 2.362(2) and 2.372(2) Å, are slightly shorter than observed in Nd(**2c**)(NO<sub>3</sub>)<sub>3</sub>, 2.390(3) and 2.378(3) Å, and the Nd–O(N) distance, 2.459(2) Å, is significantly longer than in Nd(**2c**)(NO<sub>3</sub>)<sub>3</sub>, 2.382(3) Å. The longer Nd–O(N) distance is consistent with a weaker N-oxide/Nd interaction that may be in response to electron withdrawal by the CF<sub>3</sub> groups or increased steric factors because of the presence of the large CF<sub>3</sub> groups. The P=O and N–O distances, 1.489(2), 1.493(2), and 1.329(3) Å are comparable with the related bond lengths in Nd(**2c**)(NO<sub>3</sub>)<sub>3</sub>: 1.500(3), 1.504(3), and 1.337(4) Å. These observations are consistent with the observed P=O coordination shifts in the IR spectra for Nd(**2a**)(NO<sub>3</sub>)<sub>3</sub> and the difficulty in locating a shifted N–O stretch for the new complex. Lastly, the Nd–O distances involving the nitrate groups suggest that one nitrate is symmetrically coordinated in a bidentate fashion while two are asymmetrically bonded. This may indicate that one or both of these anions might be replaced in the inner coordination sphere by another neutral molecule of **2a**. This is observed with **2c** where Nd(**2c**)(NO<sub>3</sub>)<sub>3</sub> can be converted to [Nd(**2c**)<sub>2</sub>(NO<sub>3</sub>)](NO<sub>3</sub>)<sub>2</sub>.<sup>3</sup>

**Nd(2a)(NO<sub>3</sub>)<sub>3</sub>·(CH<sub>3</sub>CN)<sub>0.5</sub>.** Combination of **2a** and Nd(NO<sub>3</sub>)<sub>3</sub> in a 2:1 ratio in the mixed solvent acetone/MeOH gave a white powder; however, attempts to recrystallize this solid from acetone or MeOH failed. On the other hand, when the initial white powder was recrystallized from CH<sub>3</sub>CN, violet crystals were obtained, and the



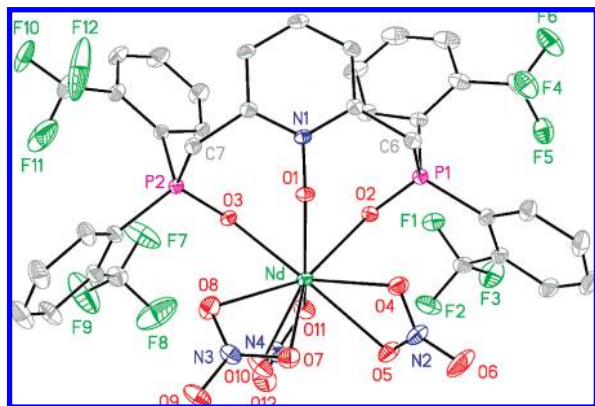


**Figure 6.** Molecular structure and atom labeling scheme for  $\text{Nd}(\mathbf{2a})(\text{NO}_3)_3 \cdot (\text{CH}_3\text{CN})_{0.5}$  (20% thermal ellipsoids; all hydrogen atoms and  $\text{CH}_3\text{CN}$  omitted for clarity).

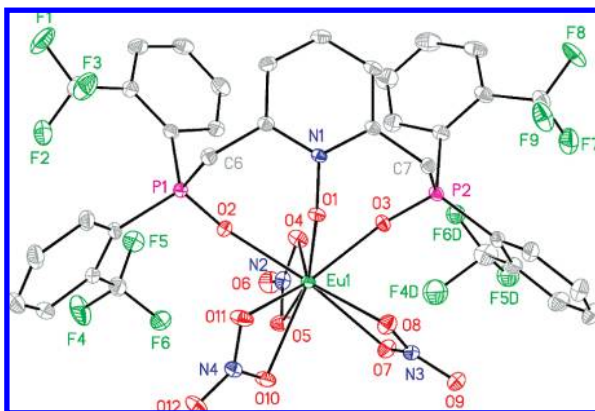


**Figure 7.** Molecular structure and atom labeling scheme for  $\text{Eu}(\mathbf{2a})(\text{NO}_3)_3$  (20% thermal ellipsoids; all hydrogen atoms omitted for clarity).

determined by X-ray diffraction methods. A view of the molecule, with the outer sphere  $\text{CH}_3\text{CN}$  omitted, is shown in Figure 6, and selected bond lengths are given in Table 2. Although the ligand/metal combining ratio is 2:1, the complex formed is 1:1 and coordination number remains 9. In this complex the coordination polyhedron more closely approximates a monocapped square antiprism. This results from more symmetrical binding of the three nitrate groups on Nd(III). This is not the only difference. Here the ligand **2a** has a shorter Nd–O(N) distance 2.385(3) Å and longer Nd–O(P) distances, 2.397(3) and 2.425(3) Å compared to the values in  $\text{Nd}(\mathbf{2a})(\text{NO}_3)_3$ .

**$\text{Eu}(\mathbf{2a})(\text{NO}_3)_3$ .** The 1:1 combination of **2a** and  $\text{Eu}(\text{NO}_3)_3$  in MeOH gave a white solid that slowly recrystallized from DMF providing single crystals of this complex. A view of the molecule is shown in Figure 7, and selected bond lengths are listed in Table 2. The structure is very similar to that found for  $\text{Nd}(\mathbf{2a})(\text{NO}_3)_3$  with a distorted nine coordinate spenoid polyhedron. The Eu–O(N) distance, 2.424(3) Å, is longer than the Eu–O(P) distances, 2.334(2) and 2.320(2) Å, and the small differences in bond lengths between the Eu and Nd complexes appear to be in line with the differences in ionic radii: Eu (C.N. = 8) 1.21 Å, Nd (C.N. = 8) 1.26 Å.

**$\text{Nd}(\mathbf{2b})(\text{NO}_3)_3 \cdot (\text{H}_2\text{O})_{1.25}$ .** The 2:1 combination of **2b** with  $\text{Nd}(\text{NO}_3)_3$  in acetone gave a white solid that was recrystallized from  $\text{CH}_2\text{Cl}_2$ . The structure determination revealed the

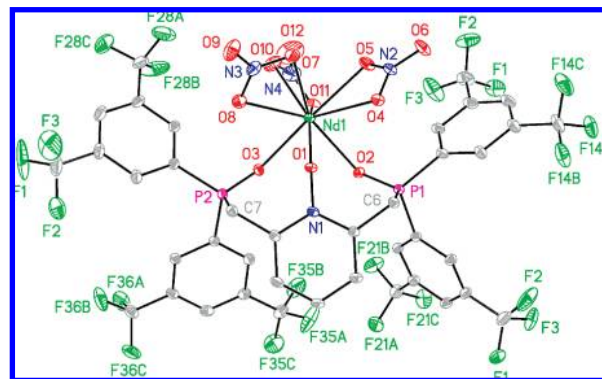


**Figure 8.** Molecular structure and atom labeling scheme for  $\text{Nd}(\mathbf{2b})(\text{NO}_3)_3 \cdot (\text{H}_2\text{O})_{1.25}$  (20% thermal ellipsoids; all hydrogen atoms and water omitted for clarity).

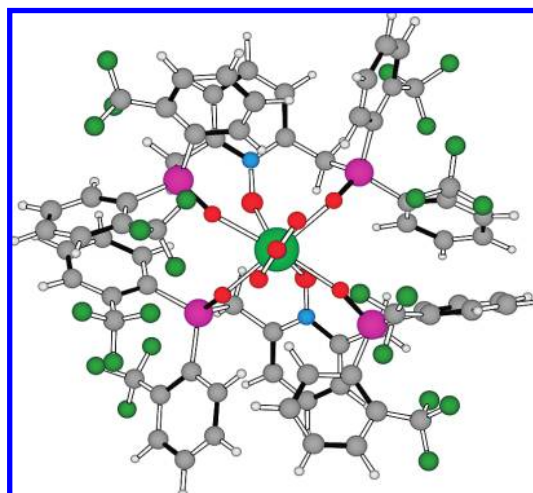


**Figure 9.** Computed structure for  $[\text{Nd}(\mathbf{2a})_2(\text{NO}_3)_3]^{+2}$ .

formation of a 1:1 complex, and a view of the molecule with the outer sphere water omitted for clarity is shown in Figure 8. Selected bond lengths appear in Table 2. The Nd polyhedron approximates a nine coordinate distorted monocapped square antiprism. The water molecule (2.5  $\text{H}_2\text{O}/2\text{Nd}$  in unit cell) is disordered along with three of the  $\text{CF}_3$  groups but this likely has no effect on the ligand binding to Nd. This structure is very similar to that described for  $\text{Nd}(\mathbf{2a})(\text{NO}_3)_3 \cdot (\text{CH}_3\text{CN})_{0.5}$  with more symmetrical binding of the nitrate anions and tighter (shorter) binding of the N–O donor group to Nd(III), 2.374(1) Å, and longer M–O(P) bond lengths, 2.457(1) and 2.396(1) Å.

## Conclusions

The trifluoromethyl phenyl decorated NOPOPO ligands have been prepared in an effort to obtain a NOPOPO-like extractant that can be used with the sulfone process solvent FS-13. Although somewhat less soluble than the CMPO extractant  $\text{Ph}_2\text{P}(\text{O})\text{CH}_2\text{C}(\text{O})\text{NBu}_2$  in FS-13, the derivative **2a** has sufficient solubility ( $\sim 0.01$  M) to encourage further study. Before undertaking that work it was important to characterize the new ligands and determine if the  $\text{CF}_3$  substituents impact the coordination of the ligands with lanthanide ions. Besides being soluble in FS-13, which is not the case with EtHx-NOPOPO, the two ligands **2a** and

**2b** are solids. This makes the purification of **2a** and **2b** much easier than for the heavy oil EtHxNOPOPO. Structural analyses indicate that the free ligands do not adopt a preferred preorganized tridentate metal binding geometry but as found with CMPO other NOPOPO ligands, the molecules are able to reorganize under mild conditions to the chelating geometry. This is confirmed by the isolation and structural characterization of four different Ln(III) 1:1 complexes. It is noted that all attempts to form 2:1 ligand/Ln complexes gave no crystalline complexes. Whether this is an outcome of reduced ligand base strength because of the CF<sub>3</sub> substituents or steric effects is not clear at this time. However, recall, vide supra, that the parent NOPOPO **1c** does form 2:1 complexes with Ln(III) ions, [Ln(**1c**)<sub>2</sub>(NO<sub>3</sub>)](NO<sub>3</sub>)<sub>2</sub>, in which two nitrate ions are displaced from the inner coordination sphere to the outer sphere, and *both* ligands **1c** are bonded in a tridentate fashion.<sup>1,3</sup> This results in coordination numbers of eight in these complexes. To potentially shed further light on the steric issue, the hypothetical molecule Nd(**2a**)<sub>2</sub>(NO<sub>3</sub>)<sub>3</sub> was modeled with an inner sphere composition, [Nd(**2a**)<sub>2</sub>(NO<sub>3</sub>)<sup>2+</sup>]; the complex is found to be sterically realistic as shown in Figure 9. Efforts will continue to isolate such 2:1 complexes under modified conditions. In addition, extraction analyses will be undertaken.

Another feature of the free ligands proved interesting. Namely, in the solid state the 2-CF<sub>3</sub> substituents on the phenyl groups interact with the backside of the P-atom in

**1a** and **2a**. It is not clear that this geometry exists in solution, but this interaction may play a role in solution thermodynamics for extraction. It is also possible that this interaction partially offsets the expected “first order” electron withdrawal of electrons by the CF<sub>3</sub> groups.<sup>46</sup>

**Acknowledgment.** Acknowledgment is made to the U.S. Department of Energy (DOE), Chemical Sciences, Geosciences and Biosciences Office, Office of Basic Energy Sciences (Grant DE-FG02-03ER15419) for financial support at UNM (R.T.P.).

**Supporting Information Available:** CIF files for the crystal structures, all-atom ORTEP plots, IR spectra and computational material. This material is available free of charge via the Internet at <http://pubs.acs.org>.

IC802390C

- 
- (46) If  $\sigma$  orbital effects dominate the electron distribution in these molecules, it would be expected that addition of CF<sub>3</sub> substituents to the phenyl groups would result in withdrawal of electron density from the P=O groups causing, for example, decreased basicity, downfield <sup>31</sup>P NMR shifts and increased  $\nu_{\text{PO}}$ . However, if one or more fluorine atoms associate with the back side of the P(V) center in solid and solution conditions, then this may offset some of this first order electron withdrawal. This would, in turn, offset shifts in <sup>31</sup>P and  $\nu_{\text{PO}}$ . Pi-electron shifts also certainly contribute in these molecules and further study will be required to provide a more detailed picture of the impacts of CF<sub>3</sub> substituents on the bonding and spectra for these and related compounds.